Research Square

Preprints are preliminary reports that have not undergone peer review.
They should not be considered conclusive, used to inform clinical practice,
or referenced by the media as validated information.

Tumor Susceptibility Gene 101 Is Required for the Maintenance of Uterine Epithelial Cells During Embryo Implantation

Hyunji Byun
Konkuk University
Sojung Kwon
Konkuk University
Kay-Uwe Wagner
Wayne State University
Hyejin Shin
Korea Institute of Oriental Medicine
Hyunjung Jade Lim (hlim@konkuk.ac.kr)
Konkuk University https://orcid.org/0000-0003-2191-666X

Research Article

Keywords: Tsg101, uterus, epithelium, implantation, necroptosis

Posted Date: March 4th, 2021

DOI: https://doi.org/10.21203/rs.3.rs-277031/v1

License: This work is licensed under a Creative Commons Attribution 4.0 International License.
Read Full License

Version of Record: A version of this preprint was published at Reproductive Biology and Endocrinology on July 16th, 2021. See the published version at https://doi.org/10.1186/s12958-021-00788-z.

Abstract

Background: The tumor susceptibility gene 101 (Tsg101), a component of the endosomal sorting complex required for transport (ESCRT) complex I, is involved in multiple biological processes involving endomembranous structures and the plasma membrane. The role of *Tsg101* in the uterine epithelium was investigated in *Tsg101* floxed mice crossed with *Lactoferrin-iCre* mice ($Tsg101^{d/d}$).

Methods: $Tsg101^{d/d}$ mice were bred with stud male mice and the status of pregnancy was examined on days 4 and 6. Histological analyses were performed to examine the uterine architecture. Immunofluorescence staining of several markers was examined by confocal microscopy. Uterine epithelial cells (UECs) were isolated from $Tsg101^{f/f}$ and $Tsg101^{d/d}$ mice, and the expression of necroptosis effectors was examined by RT-PCR, western blotting, and immunofluorescence staining. UECs were also subjected to RNA expression profiling.

Results: $Tsg101^{d/d}$ female mice were subfertile with implantation failure, showing unattached blastocysts on day 6 of pregnancy. Histological and marker analyses revealed that some $Tsg101^{d/d}$ day 4 pregnant uteri showed a disintegrated uterine epithelial structure. $Tsg101^{d/d}$ UECs began to degenerate within 18 h of culture. In UECs, expression of necroptosis effectors, such as RIPK1, RIPK3, and MLKL were first confirmed. UECs responded to a stimulus to activate necroptosis and showed increased cell death.

Conclusions: *Tsg101* deficiency in the uterine epithelium causes implantation failure, which accompanies epithelial defects. This study provides evidence that UECs harbor a necroptotic machinery that responds to death-inducing signals. Thus, Tsg101 expression in the uterine epithelium is required for normal pregnancy in mice.

Background

The endosomal sorting complex required for transport (ESCRT) complexes, ESCRT-0, -I, -II, and -III, act in sequence as key regulators of endosomal sorting and maturation. The ESCRT-I complex contains tumor susceptibility gene 101 (Tsg101), vacuolar protein sorting-associated protein 28 homolog Vsp28, Vsp37, and multivesicular body sorting factor 12 (Mvb12) proteins [1]. As a component of ESCRT-I, Tsg101 forms a complex with other ESCRT factors and is essential for the recruitment of subsequent ESCRT complexes [2]. ESCRT proteins are also required for the maintenance of epithelial cell polarity [3].

Tsg101 protein has a ubiquitin-interacting domain and downregulates ubiquitinated cell surface receptors and certain protein aggregates [4, 5]. It is also involved in cytokinesis and viral exit from infected cells [6, 7]. Systemic deletion of *Tsg101* results in early embryonic death between embryonic days 5.5 and 6.5 due to defective cell proliferation [8]. Deletion of *Tsg101* in mouse embryonic fibroblasts (MEFs) causes cell cycle arrest and cell death [9], suggesting a complex role for this gene [7].

Cell death is essential for various biological processes including basic pathophysiology and embryonic development [10]. Depending on the molecular pathways and morphological characteristics, cell death is

classified into several types, such as apoptosis, autophagy, and programmed necrosis (necroptosis) [11]. Necroptosis often begins with the activation of death receptors by cognate ligands, such as tumor necrosis factor α (TNFα), TNF related apoptosis-inducing ligand (TRAIL), and FAS ligand (FASL). Intracellular signaling follows involving receptor-interacting protein kinase (RIPK) 1, RIPK3, and mixed lineage kinase-like (MLKL) proteins [12]. Phosphorylated MLKL (pMLKL) proteins translocate to the plasma membrane and mediate membrane permeabilization [13]. MLKL activation results in Ca^{2+} influx, which is rapidly followed by lipid scrambling of the plasma membrane. The damaged plasma membrane depends on certain ESCRT components to maintain integrity following MLKL activation. Charged multivesicular body protein 4B (CHMP4B) and other ESCRT factors produce small membrane vesicles to mend the plasma membrane during necroptosis [13]. Tsg101 promotes the translocation of ESCRT-III factors to the sites of membrane damage and counteracts plasma membrane rupture during necroptosis [13].

In mice, embryo implantation occurs around midnight on day 4 of pregnancy [14]. For this process to proceed successfully, the luminal epithelium undergoes steroid hormone-induced proliferation and differentiation, which renders it competent for embryo attachment [15]. The communication between an implantation-competent blastocyst and a receptive uterus is central to the implantation process and successful pregnancy, and any defect in this process results in implantation failure [15]. The uterine epithelium at the time of embryo implantation undergoes differentiation, expressing several factors involved in two-way interactions. The importance of epithelial polarity in embryo implantation has been demonstrated in a study examining the role of planar cell polarity signaling [16].

Lactoferrin (*Ltf*) encodes a non-heme iron-binding glycoprotein and is highly responsive to estrogen in the mouse uterus [17]. *Ltf* is expressed in the uterine epithelium of adult mice but not in immature mouse uteri [18]. A mouse *Cre* model taking advantage of this expression pattern is available as *Ltf-iCre* knock-in mice [19], in which *iCre* is expressed under the endogenous *Ltf* promoter. This *Cre* model efficiently recombines the floxed target gene, primarily in the uterine epithelium, in adult female mice and immature females after estrogen treatment [19]. In this study, we generated a uterine epithelium-specific *Tsg101* deletion model by crossing *Tsg101* floxed (*Tsg101*$^{f/f}$) mice with *Ltf-iCre* mice to examine its role in this cell type. Our results show that Tsg101 is required for the maintenance of the uterine epithelium and embryo implantation.

Materials And Methods

Reagents

17β-estradiol (E_2) (Sigma-Aldrich, St. Louis, MO, USA) was dissolved in sesame oil (Acros Organics). Equine chorionic gonadotropin (eCG) and human chorionic gonadotropin (hCG) were purchased from Sigma-Aldrich.

Mice

All mice were maintained in accordance with the policies of the Konkuk University International Animal Care and Use Committee (IACUC). *Tsg101* floxed mice (*Tsg101*$^{f/f}$) mice [8] were crossed with *Ltf-iCre* mice [19] to obtain *Ltf-iCre*; *Tsg101*$^{f/f}$ (*Tsg101*$^{d/d}$) mice. *Tsg101*$^{d/d}$ mice were produced by crossing *Tsg101*$^{f/f}$ female mice with *Ltf-iCre*; *Tsg101*$^{f/d}$ male or *Ltf-iCre*; *Tsg101*$^{f/f}$ male mice. Genomic DNA was extracted from mouse tails using Gentra Puregene Mouse Tail kit (Qiagen, Hilden, Germany). Genotyping PCR for the floxed *Tsg101* and *Ltf-iCre* genes was performed using the primers shown in Table 1. This study was approved by the Konkuk University IACUC (approval number KU20036).

Table 1
Primers used for genotyping and RT-PCR analyses.

Gene	Sequence (5′–3′)	Annealing temperature (°C)	No. of cycles	Product size (bp)
Tsg101 wildtype	F: CCG TGA TCT CTT GAT TCT TCT CC R: CCT GCT CTT TAC TGA AGG CTC	58	35	482
Tsg101 floxed	F: CCG TGA TCT CTT GAT TCT TCT CC R: GAA ATC CAC CTG CCT CTG CCT C	58	35	482
Ltf^{iCre} transgene	F: AAC TAG CAC ACC TGG TTG AGG R: CAG GTT TTG GTG CAC AGT CA	60.5	10	215
Des	F: CAA AGG GGT TCT GAA GTC CA R: GAA AAG TGG CTG GGT GTG AT	59	28	198
Krt12	F: GTC TCA TCC CAG GTT CAG GA R: TGC AAT GAA GAC CAG CAG AG	59	26	231
Rpl7	F: TCA ATG GAG TAA GCC CAA AG R: CAA GAG ACC GAG CAA TCA AG	59	28	246
Tsg101	F: ATG GCG GTG TCC GAG AGT CAG R: TTG ACA GTT TGA CGG ACG GT	55	33	80
Ripk1	F: GAA GAC AGA CCT AGA CAG CGG R: CCA GTA GCT TCA CCA CTC GAC	58	35	182

Gene	Sequence (5− 3)	Annealing temperature (ºC)	No. of cycles	Product size (bp)
Ripk3	F: CAC ATA CTT TAC CCT TCA GA R: TCA GAA CAG TTG TTG AAG AC	58	35	172
Mlkl	F: GAC CAA ACT GAA GAC AAG TA R: CTC ACT ATT CCA ACA CTT TC	57	35	114
Aqp8	F: GGG GCA GCC TTT GCC ATC GT R: AAG AGG CCA GCC AGG AGG GG	59	28	296

Examination of mice on days 4 and 6 of pregnancy

Tsg101$^{f/f}$ and *Tsg101*$^{d/d}$ female mice (9 to 13-week-old) received 2.5 IU of eCG and hCG at 48 h intervals to promote mating. Immediately after hCG injection, they were bred with stud male mice. On the following morning, the formation of a vaginal plug was confirmed, and females with plugs were considered to be on day 1 of pregnancy. To examine implantation sites on day 6 of pregnancy, mice received a blue dye injection (1% Chicago blue B in phosphate buffered saline (PBS; Gibco, Thermo Fisher Scientific, Waltham, MA, USA) and sacrificed 3 min later. When no implantation site was visible, uteri were flushed with M2 medium (M7167, Sigma-Aldrich). Some mice were sacrificed at 11 AM on day 4 of pregnancy to confirm the presence of embryos. One uterine horn was flushed with M2 media and the other was processed for histological analyses.

Pseudopregnancy

Tsg101$^{f/f}$ and *Tsg101*$^{d/d}$ female mice at 10 to 11-weeks of age received 2.5 IU of eCG and hCG at 48 h intervals. Immediately after hCG injection, the mice were bred with vasectomized ICR male mice. On the following morning, the formation of a vaginal plug was confirmed and females with plugs were considered to be on day 1 of pseudopregnancy. The uteri were collected from days 1, 4, or 6 of pseudopregnancy, and used for histological analysis and immunofluorescence staining. Uteri from day 4 pseudopregnant mice were used for uterine cell preparations.

Histological analyses

The uteri from pregnant or pseudopregnant mice were cut into small pieces and fixed in 4% paraformaldehyde (PFA) in PBS overnight. Using a tissue processor, samples were dehydrated and

embedded in paraffin. Sections (6–8 μm) were made using a microtome, placed onto a glass slide, and then subjected to hematoxylin-eosin (HE) staining. Slides were then examined using an upright microscope (Eclipse 80i, Nikon, Tokyo, Japan).

Isolation of mouse uterine epithelial cells (UECs) and uterine stromal cells (USCs)

Uteri from random cycling ICR (8-week-old), *Tsg101*$^{f/f}$, or *Tsg101*$^{d/d}$ mice received a subcutaneous injection of E_2 (100 ng/0.1 ml in sesame oil) 24 h before sacrifice to induce proliferation of UECs. Uteri pooled from 3 to 5 mice were cut into 3–4 mm pieces. Pancreatin (P3292; Sigma-Aldrich), dispase (17105–041; Gibco, Thermo Fisher Scientific), and collagenase (C1639; Sigma-Aldrich) were used to isolate uterine epithelial cells (UECs) and uterine stromal cells (USCs) as previously described [20]. Isolated UECs were filtered through a 70 μm nylon mesh filter (Corning, Sigma-Aldrich) to improve purity. UECs (2×10^5 cells) were grown on collagen-coated coverslips in a 6-well plate (Corning, Sigma-Aldrich) in DMEM/F12 (Gibco, Thermo Fisher Scientific) supplemented with 10% fetal bovine serum (FBS) (Gibco, Thermo Fisher Scientific) and 1% penicillin-streptomycin (Lonza).

Cell culture and necroptosis induction

The L929 fibroblast cell line derived from mouse adipose tissue was obtained from the Korean Cell Line Bank (Seoul, Korea). L929 cells were cultured in DMEM media (11965–092, Gibco, Thermo Fisher Scientific) supplemented with 10% FBS (10099–141, Gibco, Thermo Fisher Scientific) and 1% penicillin-streptomycin (17-602E, Lonza, Basel, Switzerland). To induce necroptosis, UECs were treated with a mixture of 30 ng/mL TNF-α (PeproTech, Rocky Hill, NJ, USA), 10 μM Smac mimetic LCL-161 (R&D Systems, Minneapolis, MN, USA), and 20 μM ZVAD-FMK (R&D Systems) for 40 min [21]. Control cells were treated with 0.2% dimethyl sulfoxide (vehicle). L929 cell lysates were used as positive controls in western blotting.

RNA extraction and reverse transcription-polymerase chain reaction (RT-PCR)

Total RNA was extracted from pooled UECs and USCs isolated from several mice using the TRIzol Reagent (Invitrogen, Carlsbad, CA, USA) according to the manufacturer's protocol. RNA was treated with RQ RNase-free DNase (Promega, Madison, WI, USA) to remove any genomic DNA for 20 min at 25°C, followed by 10 min at 75°C to inactivate the DNase. RNA concentration and quality were assessed using a NanoDrop (ND-1000; Thermo Fisher Scientific). Complementary DNA (cDNA) was synthesized from RNA using MMLV reverse transcriptase (BeamsBio, Seoul, Korea) and random hexamer primers (Invitrogen). Primers used for RT-PCR analyses are listed in Table 1. *Keratin 12 (Krt12)* and *desmin (Des)* were used as markers of the uterine epithelium and stroma, respectively [22].

Western blotting

Isolated UECs and USCs were collected in RIPA buffer [10 mM Tris (pH 7.2), 150 mM NaCl, 0.1% Triton X-100, 5 mM ethylenediaminetetraacetic acid, 1% sodium dodecyl sulfate (SDS), 1 mM dithiothreitol, 1 mM phenylmethylsulfonyl fluoride, and 1X protease inhibitors) and homogenized. The lysates were centrifuged at 12,600 × g for 15 min at 4°C and the supernatants collected. A bicinchoninic acid protein assay (Thermo Fisher Scientific) was performed to determine the concentration of the extract. The lysates were prepared in 4X sample buffer and boiled for 5 min. Samples were loaded onto SDS-polyacrylamide gels and transferred onto polyvinylidene difluoride membranes (Millipore, Billerica, MA, USA). Membranes were blocked with 5% skim milk for 1 h and incubated overnight at 4°C with the primary antibodies shown in Table 2. The membranes were washed three times and then incubated with secondary antibodies (Table 2) at 25°C for 1 h. Chemiluminescence signals were detected using the West Save Detection Reagent A (Ab Frontier, Seoul, Korea) or West Femto kit (Thermo Fisher Scientific) and visualized with a LAS 4000 system (Fujifilm, Tokyo, Japan).

Table 2
Antibodies used in this study.

Antibody	Host	Cat. no	Supplier	Dilution	Application
β-tubulin	Rabbit	ab6046	Abcam	1:2000	WB
RIPK1	Mouse	610459	BD biosciences	1:500	WB/IF
pRIPK1	Rabbit	83613	Cell signaling	1:500	WB
pRIPK1	Rabbit	31122	Cell Signaling	1:1000	IF
RIPK3	Rabbit	NBP1-77299	Novus	1:500	WB/IF
pRIPK3	Rabbit	91702	Cell signaling	1:500	WB
pRIPK3	Rabbit	57220	Cell Signaling	1:1000	IF
MLKL	Rat	MABC604	Merk	1:500	WB/IF
pMLKL	Rabbit	ab196436	Abcam	1:500	WB/IF
E-cadherin	Rabbit	3195	Cell signaling	1:200	IF
MUC1	Rabbit	PA1-21077	ThermoFisher	1:200	IF
EEA1	Rabbit	2411	Cell signaling	1:250	IF
Lamp1	Rat	NB100-77683	Novus	1:125	IF
Desmin	Goat	Sc7559	Santa Cruz	1:250	IF
Anti-rabbit IgG-HRP	Goat	SA002-500	GenDEPOT	1:10000	WB
Anti-mouse IgG-HRP	Goat	SA001-500	GenDEPOT	1:10000	WB
Anti-rat IgG-HRP	Goat	62-9520	Invitrogen	1:10000	WB
Anti-rabbit IgG-Alexa Fluor 488	Chick	A21441	Invitrogen	1:250	IF
Anti-rat IgG-Alexa Fluor 488	Donkey	A21208	Invitrogen	1:250	IF
Anti-goat IgG-Alexa Fluor 488	Rabbit	A21222	Invitrogen	1:250	IF
Anti-mouse IgG-Alexa Fluor 488	Donkey	A31571	Invitrogen	1:250	IF

Immunofluorescence staining and confocal microscopy

Cells were fixed in 4% PFA for 10 min and washed three times with PBS for 3 min each. Cells were then permeabilized with 0.25% Triton X-100 for 10 min and blocked with 2% bovine serum albumin (BSA) in

PBS for 1 h at 25°C. The cells were incubated with primary antibodies overnight at 4°C. After washing, the slides were incubated with secondary antibodies at 25°C for 1 h in the dark. DNA was counter-stained with TOPRO-3-iodide (Invitrogen).

For immunofluorescence staining of uterine sections, pieces from the uteri of *Tsg101*$^{f/f}$ and *Tsg101*$^{d/d}$ mice were fixed in 4% PFA in PBS overnight, followed by 30% sucrose solution overnight. The tissues were then frozen in optimal cutting temperature compound (Leica Biosystems, Wetzlar, Germany) with instant freezing aerosol. Sections (12 μm) were made using a cryostat (Leica Biosystems). The frozen sections were fixed in 4% PFA and permeabilized with 0.1% Tween-20 at 25°C for 20 min. After blocking with 2% BSA in PBS for 1 h at 25°C, the sections were incubated with primary antibodies overnight at 4°C. After washing, the slides were incubated with secondary antibodies at 25°C for 1 h in the dark. DNA was counter-stained with TOPRO-3-iodide. Images were obtained with a Zeiss LSM900 confocal microscope (Carl Zeiss AG, Oberkochen, Germany) and analyzed with the ZEN Blue software (Carl Zeiss AG). Primary and secondary antibodies are shown in Table 2.

TUNEL assay

Apoptosis was analyzed using the DeadEnd Fluorometric terminal deoxynucleotidyl transferase-mediated dUDP nick end labeling (TUNEL) assay kit (G3250; Promega). Paraffin sections of day 4 pseudopregnant uteri were deparaffinized in xylene, rehydrated through a graded series of ethanol, and washed with PBS. The sections were fixed in 4% PFA for 25 min and then permeabilized with 0.1% Triton X-100 for 5 min. The slides were equilibrated with equilibration buffer for 10 min and then incubated with recombinant terminal deoxynucleotidyl transferase incubation buffer at 37°C for 1 h and covered with plastic coverslips. Sections were incubated with 2X SCC buffer for 15 min and washed with PBS three times. The sections were counter-stained with TO-PRO-3-iodide (1:250 in PBS) for 15 min at 25°C in the dark and rinsed three times in PBS for 5 min each. The slides were mounted in antifade reagent (Invitrogen), examined under a Zeiss LSM900 confocal microscope and analyzed with the ZEN Blue software.

Live imaging during UEC culture

Isolated UECs were cultured in 60 mm dishes in culture medium. The cells were placed under a JuLI™ FL time-lapse microscope (JuLI-B004, NanoEntek, Seoul, Korea) in a CO_2 incubator. For activation of necroptosis, TNF-α (30 ng/mL), Smac mimetic LCL161 (10 μM), and z-VAD (20 μM) were added to the culture media as described above. UECs were stained with SYTOX™ Green Nucleic Acid Stain (S7020, Invitrogen) and imaged automatically at 1 h intervals.

RNA expression profiling

To compare the RNA expression profiles between *Tsg101*$^{f/f}$ and *Tsg101*$^{d/d}$ UECs, uteri from 3 *Tsg101*$^{f/f}$ or 4 *Tsg101*$^{d/d}$ mice were pooled and RNA extracted (n = 3 for each group). RNA quality was assessed using the 2100 Bioanalyzer system (Agilent Technologies, Santa Clara, CA, USA). Total RNA (1 μg) obtained from the samples was used for RNA extraction with the MGIEasy RNA Directional Library Prep Kit (LAS, Gimpo, Gyeonggi-do, Korea) and processed for high-throughput sequencing using MGISEQ-2000. Volcano

plots for the expression-fold changes and p-values between the two selected samples were plotted by in-house R scripts. The top differentially expressed genes (DEGs) with ≥ 2-fold change ($p \leq 0.05$) are shown as a heatmap, also drawn by an in-house R script. Significant changes in the biological processes based on Gene Ontology (GO), Kyoto Encyclopedia of Genes and Genomes (KEGG) pathways, and other functional gene sets were analyzed by g:Profiler version 0.6.7 [23].

Statistical analysis

Graphing and data analysis were performed using GraphPad Prism 5 software (https://www.graphpad.com/scientific-software/prism/) (Graph Pad Software, San Diego, CA, USA).

Results

Generation of uterine epithelium-specific *Tsg101* deletion model

The uterine epithelium-specific deletion of Tsg101 was achieved by crossing *Tsg101*$^{f/f}$ mice [8] with *Ltf-iCre* mice [19]. Deletion of *Tsg101* in isolated UECs, but not in the uterine stromal cells (USCs), was confirmed by RT-PCR (Fig. 1A).

Implantation failure in *Tsg101*$^{d/d}$ mice on day 6 of pregnancy

Tsg101$^{d/d}$ female mice were bred with stud male mice for several months, however, they did not produce any pups. The status of pregnancy in the *Tsg101*$^{d/d}$ mice was examined on day 6 of pregnancy when implantation sites (IS) are generally visible. As shown in Fig. 1B, 6 out of 7 pregnant *Tsg101*$^{d/d}$ mice showed no IS, whereas control mice showed evenly spaced IS. The uterine flushings of *Tsg101*$^{d/d}$ uteri (4 out of 8 mice), showed unimplanted, zona-free blastocysts (Fig. 1B & D). *Tsg101*$^{d/d}$ uteri on day 6 showed variable thickness, as shown in Fig. 1B. Notably, the entire or portion of the uterus in some *Tsg101*$^{d/d}$ mice showed water imbibition (see Fig. 1B). Uterine histology of *Tsg101*$^{d/d}$ mice showed that the overall uterine architecture was normal, with all major cell types and glands visible (Fig. 1D). However, no luminal closure or decidualization was observed on day 6, suggesting that the implantation reaction was not initiated.

Delayed embryonic development in *Tsg101*$^{d/d}$ uteri on day 4 of pregnancy

We next examined if embryonic development proceeds normally to the blastocyst stage by day 4 of pregnancy in *Tsg101*$^{d/d}$ mice when the uterus is receptive to implantation. One uterine horn of *Tsg101*$^{f/f}$ and *Tsg101*$^{d/d}$ mice was flushed on day 4 of pregnancy, and the developmental stage of the embryos was monitored (Fig. 2, Table 3). At 11 AM on day 4, most embryos (81.25%) from *Tsg101*$^{f/f}$ mice were at the blastocyst stage, whereas only 43.3% of the embryos from the *Tsg101*$^{d/d}$ uteri were at the same stage (Table 3). These results show that embryonic development in *Tsg101*$^{d/d}$ mice is marginally delayed. Nonetheless, the presence of blastocysts on day 4 in *Tsg101*$^{d/d}$ mice, which failed to implant by day 6 of pregnancy was confirmed (Fig. 1B).

Table 3
The number of embryos in uterine flushings of day 4 pregnant mice.

Genotype	No. of plug-positive mice	No. of mice with embryos	Total no. of embryos*	Total no. of blastocysts (%)	Total no. of morula (%)
Tsg101$^{f/f}$	8	6	32	26 (81.25)	6 (18.75)
Tsg101$^{d/d}$	9	6	30	13 (43.3)	17 (56.7)

* Mice received 2.5 IU of eCG followed by 2.5 IU hCG 48 h later and were individually caged with stud males to induce mating. The next morning, a mouse with a visible vaginal plug was designated to be on day 1 of pregnancy. Mice were sacrificed at 11 AM on day 4. One uterine horn from each mouse was flushed and the other horn was subjected to histological analysis.

The unflushed uterine horn was subjected to histological analysis (Fig. 2B). The overall uterine structures in *Tsg101*$^{d/d}$ mice appeared normal, but the luminal epithelium seemed shorter (Fig. 2B, arrowheads and graph). Overall histological analyses suggested that the luminal epithelia of *Tsg101*$^{d/d}$ uteri on day 4 of pregnancy was less developed than those of *Tsg101*$^{f/f}$ uteri, displaying shortened heights. The average height of the luminal epithelium in *Tsg101*$^{d/d}$ uteri was approximately 30 μm, about 20% lower than that of the *Tsg101*$^{f/f}$ uteri (average 37 μm). This observation suggests that epithelial differentiation, which occurs during preparation for implantation, requires Tsg101 for structural integrity. E-cadherin and desmin, markers of the epithelium and stroma, respectively, showed an expected pattern of localization in *Tsg101*$^{d/d}$ uteri, with E-cadherin in the uterine epithelium and desmin in the stroma (Fig. 2C).

Molecular and cellular characteristics of UECs change in the absence of *Tsg101*

In early pregnancy, the status of steroid hormones fluctuates depending on the day of pregnancy [14]. On day 1 of pregnancy, when preovulatory estrogen is dominant, the uterine epithelium proliferates extensively. On day 4, progesterone levels increase and a small amount of estrogen is secreted, driving epithelial differentiation and stromal proliferation in the uterus. On day 6 of pregnancy, when implantation has already taken place, the primary hormone modulating the uterus is progesterone secreted from corpora lutea [14]. To examine the status of the uterine epithelium under different hormonal profiles, we examined E-cadherin localization on days 1, 4, and 6 of pseudopregnancy in *Tsg101*$^{f/f}$ and *Tsg101*$^{d/d}$ mice. As shown in Fig. 3A, E-cadherin was localized to the uterine epithelium in both groups. Noticeably, a chunk of epithelial mass detached from the luminal epithelium was seen in pseudopregnant some day 1 *Tsg101*$^{d/d}$ uteri. In day 4 pseudopregnant *Tsg101*$^{d/d}$ uteri, some detached cells were also observed inside the lumen. The uterine epithelium on day 6 of pseudopregnancy showed E-cadherin localization. As indicated with arrowheads, the apical side of the luminal epithelium from day 4 pseudopregnant *Tsg101*$^{d/d}$ mice appeared shorter than that of wild-type mice. We examined the localization of MUC1, a marker of apical side of the uterine epithelium [24]. In day 4 pseudopregnant *Tsg101*$^{d/d}$ uteri, MUC1 showed a normal pattern in the apical surface (Fig. 3B, left panels). In another *Tsg101*$^{d/d}$ mouse, the luminal epithelium was disorganized and collapsed (Fig. 3B) but retained E-

cadherin and MUC1 localization. Thus, the uterine epithelium retained its epithelial characteristics with intact marker expression but lost partial structural integrity. These results suggest that implantation failure in *Tsg101*$^{d/d}$ mice is associated with epithelial defects in the absence of *Tsg101*.

Cultured *Tsg101*$^{d/d}$ UECs show a high rate of degeneration

It has been previously shown that MEFs [8] and primary mammary epithelial cells [9] with *Tsg101* knockdown show poor survival and various subcellular abnormalities. Thus, UECs isolated from *Tsg101*$^{d/d}$ uteri were cultured in vitro and cell survival was monitored. We observed that *Tsg101*$^{d/d}$ UECs began to degenerate within 18 h of culture (Fig. 4A). After 72 h, the number of remaining *Tsg101*$^{d/d}$ cells was much lower than *Tsg101*$^{f/f}$ UECs and stained positive for SYTOX Green stain, which stains cells with compromised plasma membranes (Fig. 4B).

The main function of Tsg101 is correlated with cytokinesis, endosomal trafficking, and the formation of the late endosomal structures called MVBs [25]. Therefore, we examined whether endolysosomal structures in *Tsg101*$^{d/d}$ UECs were normal. Localization of early endosome antigen 1 (EEA1) and lysosome-associated membrane protein 1 (LAMP1) was examined by immunofluorescence staining (Fig. 4C). As shown in Fig. 4C, both EEA1 and LAMP1 exhibited puncta-like localization mostly in the perinuclear region, which did not differ between the *Tsg101*$^{f/f}$ and *Tsg101*$^{d/d}$ UECs. These results collectively suggest that cultured UECs tend to degenerate in the absence of Tsg101 without noticeable endolysosomal defects. Thus, increased UEC death could be associated with implantation failure in *Tsg101*$^{d/d}$ mice.

Expression of necroptosis factors in UECs

Another role for Tsg101 and other ESCRT factors has recently been suggested which involves counteracting necroptotic cell death [13]. Necroptosis can be induced by various external and internal stimuli, and the resulting plasma membrane breach is generally mediated by the RIPK1-RIPK3-MLKL pathway [11]. Whether UECs express such necroptosis effectors has not been reported. We examined the expression of these factors by RT-PCR and western blotting (Fig. 5A & B). We confirmed the expression of *Ripk1*, *Ripk3*, and *Mlkl* in isolated UECs and USCs.

In various cell types, RIPK1, RIPK3, and MLKL respond to necroptosis-inducing signals and undergo phosphorylation [12]. In L929 mouse fibroblast cells, combined treatment with TNFα (T), LCL161 (S, a Smac mimetic), and zVAD-fmk (Z, an apoptosis inhibitor) induced the phosphorylation of these three factors [21]. Using TSZ-treated L929 cells as a positive control, we examined the status of RIPK1, RIPK3, MLKL, and their phosphorylated forms by western blotting. As shown in Fig. 5B, all three factors were present in both UECs and USCs. Since their phosphorylated forms were also detected in UECs and USCs without external stimulation, it is possible that a basal level of necroptosis may be operative in these cells. Immunofluorescence staining of these factors mostly showed a scattered punctate pattern in the

cytoplasm. As for phosphorylated MLKL (pMLKL), it was localized in some UECs in the plasma membrane, which is known to occur upon activation of necroptosis (Fig. 5C, white arrowhead) [26].

We then tested whether UECs respond to exogenous necroptosis-inducing signals. UECs were treated with TSZ for 24 h in the presence of the SYTOX Green live dye. As shown in Fig. 5D, TSZ treatment dramatically increased SYTOX Green-positive UEC cells. Thus, UECs are equipped with necroptosis effectors and can respond to necroptosis-inducing exogenous signals.

Cell death in *Tsg101$^{d/d}$* UECs

The final executor of necroptosis is pMLKL, which induces permeabilization of the plasma membrane [12]. Whether the luminal epithelium expresses active pMLKL during pregnancy is unknown. We examined whether pMLKL is localized to the luminal epithelium on day 4 of pseudopregnancy (Fig. 6A). In the *Tsg101$^{f/f}$* uteri, pMLKL showed a punctate localization in a portion of the apical surface of the luminal epithelium (Fig. 6A). In the *Tsg101$^{d/d}$* uteri with shortened luminal epithelium, the pMLKL signal was not as distinct as in the *Tsg101$^{f/f}$* uteri.

To investigate whether detachment of cells in the *Tsg101$^{d/d}$* uterus is associated with apoptosis, we performed TUNEL staining on day 4 pseudopregnant uterine sections (Fig. 6B). Again, we found cells detached from the luminal epithelium and a higher number of TUNEL-positive cells in the subepithelial stromal regions in the *Tsg101$^{d/d}$* uterus.

mRNA expression landscape in the *Tsg101$^{f/f}$* and *Tsg101$^{d/d}$* UECs

To compare the overall mRNA expression landscape between the *Tsg101$^{f/f}$* and *Tsg101$^{d/d}$* UECs, we performed mRNA expression profiling. To avoid mRNA contamination from the embryos, UECs from day 4 pseudopregnant mice were used. These samples were subjected to mRNA expression profiling. Heatmaps of the top 50 differentially expressed genes (DEGs) are shown in Fig. 7A. Remarkably, genes upregulated in the *Tsg101$^{d/d}$* UECs exhibited high variation between the samples (Fig. 7A, left panel), whereas genes downregulated in *Tsg101$^{d/d}$* UECs showed a more consistent trend (Fig. 7A, right panel). In total, 1284 genes were differentially expressed between *Tsg101$^{f/f}$and Tsg101$^{d/d}$* UECs. Of these DEGs, 734 genes were upregulated, whereas 550 genes were downregulated in *Tsg101$^{d/d}$*. Histological examination of day 4 pseudopregnant uteri from some *Tsg101$^{d/d}$* mice used in this experiment showed patches of cells in the lumen (Fig. 7B). One of the downregulated gene in *Tsg101$^{d/d}$* UEC, *Aquaporin 8* (*Aqp8*), indeed were shown decreased in these samples (Fig. 7C). Fluid accumulation we had observed in several *Tsg101$^{d/d}$* uteri (Fig. 1B) may be associated with aberrant expression of water channel genes [27].

GO term enrichment and KEGG pathway analyses were used to identify key genes and pathways operative in *Tsg101$^{f/f}$* and *Tsg101$^{d/d}$* UECs (Fig. 8). In terms of DEGs in GO term enrichment analysis for the biological process (Fig. 8A), several gene classes associated with immune functions were upregulated in *Tsg101$^{d/d}$* UECs. KEGG pathway analysis of the DEGs showed clustering of several

signaling pathways, such as cell adhesion molecules and cytokine-cytokine receptor interaction (Fig. 8B). Together, these results suggest that various cellular functions were affected in the uterine epithelium in the absence of *Tsg101*.

Discussion

Tsg101 was initially cloned as a candidate tumor suppressor gene in mice [28]. While several reports suggest a role for this gene in tumor suppression [7], other complex and fundamental roles for Tsg101 in cells have been uncovered, ranging from endolysosomal maturation, cytokinesis, cell proliferation, and survival [7]. As the deletion of *Tsg101* in mice is lethal early in development [8], the biological functions of Tsg101 have been investigated in several tissue-specific *Tsg101* deletion mouse models [7]. In mammary epithelial cells, cardiomyocytes, and oligodendroglia, *Tsg101* deletion leads to cell death accompanied by apoptosis, vacuolation, and other subcellular changes [29–31].

Our study shows that Tsg101 plays a crucial role in maintaining the integrity of the uterine epithelium during embryo implantation. The *Ltf-iCre* mice achieved efficient and specific deletion of the floxed genes in the uterine epithelium at approximately 2 months of age [19]. All mice used in our experiments were between 8–11-weeks of age. By this time, all uterine structures have formed and sexual maturation is complete. Thus, the subfertility phenotype observed in $Tsg101^{d/d}$ mice is irrelevant to anatomical and endocrinological abnormalities. Our results show that *Tsg101* is required in the uterine epithelium to initiate embryo implantation (Fig. 1). The presence of well-formed, zona-free blastocysts in day 6 pregnant $Tsg101^{d/d}$ uteri suggests that the luminal epithelium is unable to support implantation.

On day 4 of pregnancy, $Tsg101^{d/d}$ uteri contained preimplantation embryos at the morula and blastocyst stages (Fig. 2A). It is unclear whether *Tsg101* deletion in the uterus is directly or indirectly associated with delayed embryonic development on day 6 (Table 3). On this day, the uterus is under the influence of progesterone and estrogen, both of which influence dynamic cellular and molecular changes required for implantation [32]. In some $Tsg101^{d/d}$ mice at 10–11-weeks of age, the luminal epithelia showed a disorganized pattern and height shortening (Fig. 3A, arrowheads). Patches of cells were also found in the uterine lumen of some $Tsg101^{d/d}$ mice. While E-cadherin and MUC-1, markers of the epithelium, exhibited normal localization in the epithelium, these markers helped identify the collapsed epithelial structure in some $Tsg101^{d/d}$ mice (Fig. 3B). When UECs were isolated and cultured in vitro, $Tsg101^{d/d}$ UECs began to show signs of degeneration around 24 h with the emergence of clustered cell patches (Fig. 4), which are uncharacteristic of epithelial cells. $Tsg101^{d/d}$ UECs also showed increased cell permeabilization, as was previously observed in certain ESCRT factor-depleted cells [13]. It was previously shown that *Tsg101*-depleted MEFs showed enlarged lysosomal structures, along with other complex cellular changes [9]. In the UECs, we did not observe a similar pattern. In vertebrate epithelial cells, ESCRT factors have been implicated in the maintenance of polarity [3]. Considering that MEFs are of mesenchymal origin, Tsg101 and other ESCRT factors may play distinct roles depending on the cell type.

Necroptosis can be initiated by various stimuli, such as death ligands and bacterial toxins, but can also be induced during normal physiological conditions and aging [12, 33]. Here, we show for the first time that UECs express the major necroptosis effectors, RIPK1, RIPK3, and MLKL, and their phosphorylated forms (Fig. 5C, arrowhead). pMLKL localization to the cell edge (Fig. 5C) suggests that UECs show active necroptosis [13, 34]. When TSZ was used to induce necroptosis [21], UECs showed a dramatic increase in SYTOX Green staining, which further supports the notion that UECs respond to external stimuli and activate necroptosis. Consistent with this finding, the *Tsg101*$^{f/f}$ uterine epithelium on day 4 of pregnancy showed a distinct punctate pattern of pMLKL localization on the epithelial edge (Fig. 6A). The presence of pMLKL implies active necroptosis involving the cell membrane. Thus, our results suggest that UECs harbor a functional necroptotic machinery. The degeneration of cultured *Tsg101*$^{d/d}$ UECs and disintegration of the uterine epithelium in *Tsg101*$^{d/d}$ uteri may be associated with a failure to counteract the necroptotic activation that occurs as a part of the normal physiology of these cells.

Finally, we compared RNA expression profiles between the *Tsg101*$^{f/f}$ and *Tsg101*$^{d/d}$ UECs (Fig. 7&8), but the RNA expression among the different *Tsg101*$^{d/d}$ UEC samples tended to show a high variation. Such high variation precluded us from pinpointing target pathways and genes associated with Tsg101 in the uterine epithelium. This could be partially due to epithelial disintegration in some *Tsg101*$^{d/d}$ mice (Fig. 3B), highlighting the importance of Tsg101 in maintaining uterine tissue architecture.

Conclusions

To date, the role of necroptosis and ESCRT factors in regulating uterine physiology and embryo implantation is not known. We confirm, for the first time, the presence of necroptosis effectors in UECs. UECs also responded to an exogenous necroptosis-inducing stimulus, involving a combination of TNFα, Smac mimetics, and an apoptosis inhibitor, and showed increased membrane permeabilization. However, *Tsg101*$^{d/d}$ UECs degenerated in vitro, even in the absence of such external stimuli. Thus, it is reasonable to assume that Tsg101 is required to sustain the survival of cultured UECs. Since UECs showed a tendency to disintegrate within *Tsg101*$^{d/d}$ uteri in vivo, it would be interesting to investigate how the tissue architecture of the uterus is maintained in older *Tsg101*$^{d/d}$ mice. Whether the uterine epithelium degenerates completely or cells of a different origin replace the epithelium in the *Tsg101*$^{d/d}$ uteri, requires further investigation. Our model can be further applied to study cell-to-cell interactions during uterine regeneration. The regulation of necroptosis in UECs and its role in uterine physiology warrants further investigation. How this cell death mechanism is related to inflammation-associated uterine pathology is another relevant topic that needs to be pursued in the future.

Abbreviations

ESCRT: Endosomal sorting complex required for transport

Tsg101: Tumor susceptibility gene 101

eCG: equine chorionic gonadotropin

hCG: human chorionic gonadotropin

MLKL: Mixed lineage kinase-like protein

RIPK1: Receptor interacting protein kinase 1

RIPK3: Receptor interacting protein kinase 3

Declarations

Ethics approval and Consent to participate

Not applicable.

Consent for publication

Not applicable.

Availability of supporting data

Data supporting the findings are presented within the manuscript.

Competing interests

The authors declare that they have no competing interests.

Funding

This work was supported by the National Research Foundation of Korea (NRF) grants (NRF-2020R1A2C1004122 and 2018R1D1A1B07045205) funded by the Korea government (MSIT). The maintenance of the *Tsg101* mutant mice was supported, in part, by the Public Health Service grant CA219332 (to K.-U.W.). The funders had no role in the study design, data collection, analysis, decision to publish, or preparation of the manuscript.

Authors' contributions

H.B., S.K., H.S., and H.J.L. devised the study; H.B., S.K., and H.S. performed the experiments; H.B., S.K., H.S., K-U. W. and H.J.L. analyzed the data; H.B. and H.J.L. wrote the manuscript with input from all authors.

Acknowledgments

The authors thank members of the Lim laboratory for their constant support. *Lft-iCre* mice were generously provided by Dr. S. K. Dey (Cincinnati Children's Hospital Research Center).

References

1. Vietri M, Radulovic M, Stenmark H: The many functions of ESCRTs. *Nat Rev Mol Cell Biol* 2020, 21:25-42.
2. Hurley JH: ESCRTs are everywhere. *EMBO J* 2015, 34:2398-2407.
3. Dukes JD, Fish L, Richardson JD, Blaikley E, Burns S, Caunt CJ, Chalmers AD, Whitley P: Functional ESCRT machinery is required for constitutive recycling of claudin-1 and maintenance of polarity in vertebrate epithelial cells. *Mol Biol Cell* 2011, 22:3192-3205.
4. Sundquist WI, Schubert HL, Kelly BN, Hill GC, Holton JM, Hill CP: Ubiquitin recognition by the human TSG101 protein. *Mol Cell* 2004, 13:783-789.
5. Bache KG, Brech A, Mehlum A, Stenmark H: Hrs regulates multivesicular body formation via ESCRT recruitment to endosomes. *J Cell Biol* 2003, 162:435-442.
6. Kumar B, Dutta D, Iqbal J, Ansari MA, Roy A, Chikoti L, Pisano G, Veettil MV, Chandran B: ESCRT-I Protein Tsg101 Plays a Role in the Post-macropinocytic Trafficking and Infection of Endothelial Cells by Kaposi's Sarcoma-Associated Herpesvirus. *PLoS Pathog* 2016, 12:e1005960.
7. Ferraiuolo RM, Manthey KC, Stanton MJ, Triplett AA, Wagner KU: The Multifaceted Roles of the Tumor Susceptibility Gene 101 (TSG101) in Normal Development and Disease. *Cancers (Basel)* 2020, 12.
8. Wagner KU, Krempler A, Qi Y, Park K, Henry MD, Triplett AA, Riedlinger G, Rucker III EB, Hennighausen L: Tsg101 is essential for cell growth, proliferation, and cell survival of embryonic and adult tissues. *Mol Cell Biol* 2003, 23:150-162.
9. Morris CR, Stanton MJ, Manthey KC, Oh KB, Wagner KU: A knockout of the Tsg101 gene leads to decreased expression of ErbB receptor tyrosine kinases and induction of autophagy prior to cell death. *PLoS One* 2012, 7:e34308.
10. Fuchs Y, Steller H: Live to die another way: modes of programmed cell death and the signals emanating from dying cells. *Nature Reviews Molecular Cell Biology* 2015, 16:329-344.
11. Green DR: The Coming Decade of Cell Death Research: Five Riddles. *Cell* 2019, 177:1094-1107.
12. Grootjans S, Vanden Berghe T, Vandenabeele P: Initiation and execution mechanisms of necroptosis: an overview. *Cell Death Differ* 2017, 24:1184-1195.
13. Gong YN, Guy C, Olauson H, Becker JU, Yang M, Fitzgerald P, Linkermann A, Green DR: ESCRT-III Acts Downstream of MLKL to Regulate Necroptotic Cell Death and Its Consequences. *Cell* 2017, 169:286-300.e216.
14. Cha J, Lim H, Dey SK: Chapter 38. Embryo Implantation. In *Knobil and Neill's Physiology of Reproduction, 4th edition.* Edited by Plant TM, Zeleznik AJ: Elsevier; 2015: 1697-1739
15. Cha J, Sun X, Dey SK: Mechanisms of implantation: strategies for successful pregnancy. *Nat Med* 2012, 18:1754-1767.
16. Yuan J, Cha J, Deng W, Bartos A, Sun X, Ho HH, Borg JP, Yamaguchi TP, Yang Y, Dey SK: Planar cell polarity signaling in the uterus directs appropriate positioning of the crypt for embryo implantation.

Proc Natl Acad Sci U S A 2016, 113:E8079-E8088.

17. McMaster MT, Teng CT, Dey SK, Andrews GK: Lactoferrin in the mouse uterus: analyses of the preimplantation period and regulation by ovarian steroids. *MolEndocrinol* 1992, 6:101-111.
18. Teng CT, Beard C, Gladwell W: Differential Expression and Estrogen Response of Lactoferrin Gene in the Female Reproductive Tract of Mouse, Rat, and Hamster. *Biology of Reproduction* 2002, 67:1439-1449.
19. Daikoku T, Ogawa Y, Terakawa J, Ogawa A, DeFalco T, Dey SK: Lactoferrin-iCre: a new mouse line to study uterine epithelial gene function. *Endocrinology* 2014, 155:2718-2724.
20. Chung D, Das SK: Mouse primary uterine cell coculture system revisited: ovarian hormones mimic the aspects of in vivo uterine cell proliferation. *Endocrinology* 2011, 152:3246-3258.
21. He S, Wang L, Miao L, Wang T, Du F, Zhao L, Wang X: Receptor interacting protein kinase-3 determines cellular necrotic response to TNF-alpha. *Cell* 2009, 137:1100-1111.
22. Choi S, Shin H, Song H, Lim HJ: Suppression of autophagic activation in the mouse uterus by estrogen and progesterone. *Journal of Endocrinology* 2014, 221:39-50.
23. Reimand J, Arak T, Adler P, Kolberg L, Reisberg S, Peterson H, Vilo J: g:Profiler-a web server for functional interpretation of gene lists (2016 update). *Nucleic Acids Res* 2016, 44:W83-89.
24. Kim HR, Kim YS, Yoon JA, Yang SC, Park M, Seol DW, Lyu SW, Jun JH, Lim HJ, Lee DR, Song H: Estrogen induces EGR1 to fine-tune its actions on uterine epithelium by controlling PR signaling for successful embryo implantation. *FASEB J* 2018, 32:1184-1195.
25. Doyotte A: Depletion of TSG101 forms a mammalian `Class E' compartment: a multicisternal early endosome with multiple sorting defects. *Journal of Cell Science* 2005, 118:3003-3017.
26. Cai Z, Jitkaew S, Zhao J, Chiang HC, Choksi S, Liu J, Ward Y, Wu LG, Liu ZG: Plasma membrane translocation of trimerized MLKL protein is required for TNF-induced necroptosis. *Nat Cell Biol* 2014, 16:55-65.
27. Zhang Y, Chen Q, Zhang H, Wang Q, Li R, Jin Y, Wang H, Ma T, Qiao J, Duan E: Aquaporin-dependent excessive intrauterine fluid accumulation is a major contributor in hyper-estrogen induced aberrant embryo implantation. *Cell Res* 2015, 25:139-142.
28. Li L, Cohen SN: Tsg101: a novel tumor susceptibility gene isolated by controlled homozygous functional knockout of allelic loci in mammalian cells. *Cell* 1996, 85:319-329.
29. Carstens MJ, Krempler A, Triplett AA, Van Lohuizen M, Wagner KU: Cell cycle arrest and cell death are controlled by p53-dependent and p53-independent mechanisms in Tsg101-deficient cells. *J Biol Chem* 2004, 279:35984-35994.
30. Essandoh K, Deng S, Wang X, Jiang M, Mu X, Peng J, Li Y, Peng T, Wagner KU, Rubinstein J, Fan GC: Tsg101 positively regulates physiologic-like cardiac hypertrophy through FIP3-mediated endosomal recycling of IGF-1R. *FASEB J* 2019, 33:7451-7466.
31. Walker WP, Oehler A, Edinger AL, Wagner KU, Gunn TM: Oligodendroglial deletion of ESCRT-I component TSG101 causes spongiform encephalopathy. *Biol Cell* 2016, 108:324-337.

32. Wang H, Dey SK: Roadmap to embryo implantation: clues from mouse models. *NatRevGenet* 2006, 7:185-199.
33. Um DE, Shin H, Park D, Ahn JM, Kim J, Song H, Lim HJ: Molecular analysis of lipid uptake- and necroptosis-associated factor expression in vitrified-warmed mouse oocytes. *Reprod Biol Endocrinol* 2020, 18:37.
34. Park HH, Park SY, Mah S, Park JH, Hong SS, Hong S, Kim YS: HS-1371, a novel kinase inhibitor of RIP3-mediated necroptosis. *Exp Mol Med* 2018, 50:125.

Figures

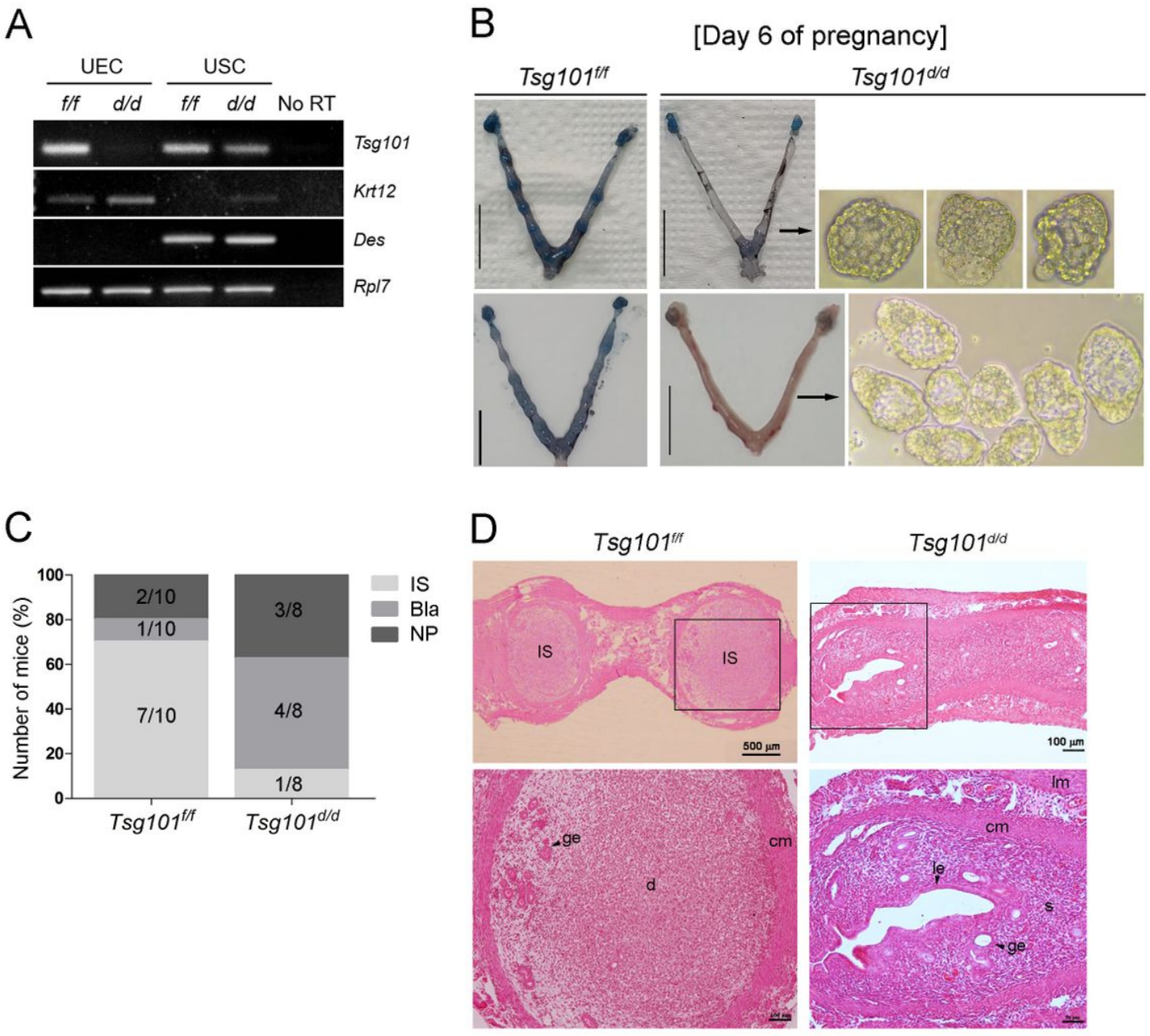

Figure 1

Compromised implantation in day 6 pregnant Ltf-iCre/Tsg101f/f mice. (A) Uterine epithelium-specific deletion of floxed Tsg101 gene by Ltf-iCre recombinase was confirmed by RT-PCR. Uterine epithelial cells (UECs) and uterine stromal cells (USCs) were isolated from 8–10-week-old random cycling Tsg101f/f or Ltf-iCre/Tsg101f/f (Tsg101d/d) mice. Deletion of Tsg101 in Tsg101d/d UECs was confirmed. Keratin 12 (Krt12) and desmin (Des) were used as marker genes for UECs and USCs, respectively. Ribosomal protein L7 (Rpl7) is a housekeeping gene and was used as an internal control. (B) Uteri of day 6 pregnant Tsg101f/f or Tsg101d/d mice. Mice (10–11-week-old) received 2.5 IU of eCG and hCG and were bred with stud male mice. On day 6 of pregnancy, the mice received a blue dye injection to demarcate the implantation sites (IS). Uteri from mice without IS were flushed. Scale bar, 1 cm. (C) Tsg101f/f (n=10) or Tsg101d/d (n=8) with variable pregnancy outcomes on day 6. Most of the Tsg101f/f mice had IS (average number = 13.3), whereas 50% of the Tsg101d/d mice showed unimplanted blastocysts upon uterine flushing. IS, mice with implantation sites; Bla, mice with unimplanted blastocysts; NP, not pregnant. (D) Histological analysis of day 6 pregnant uterine sections. Paraffin-embedded sections were stained with hematoxylin and eosin. IS, implantation site; ge, glandular epithelium; cm, circular muscle; lm, longitudinal muscle; le, luminal epithelium; s, stroma. Areas demarcated with a black square are magnified in the lower panels.

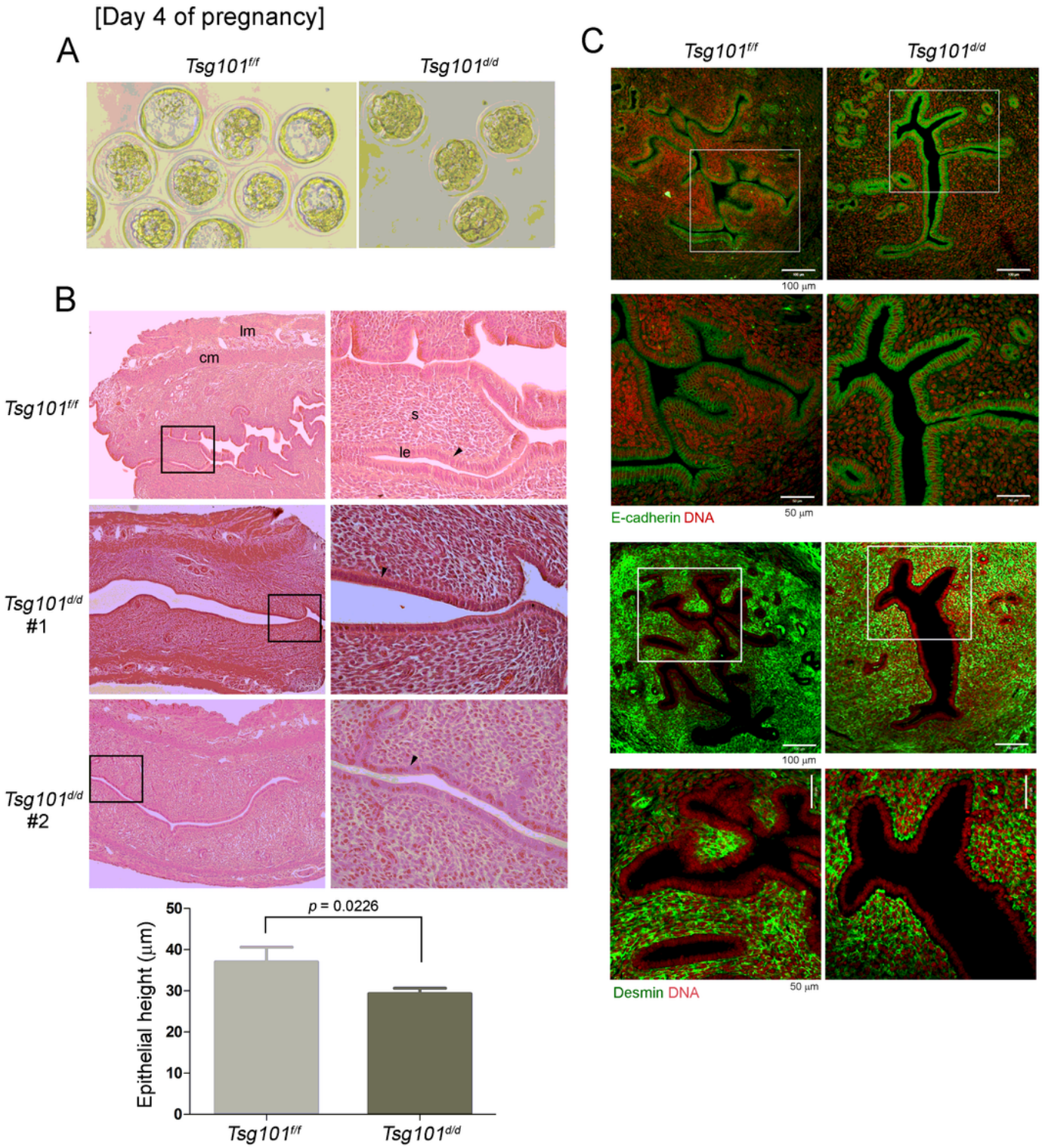

Figure 2

Day 4 pregnancy in Tsg101d/d mice. (A) Mice (10–11-week-old) received 2.5 IU of eCG and hCG and were bred with stud male mice. On day 4 at 11 AM, the uteri were collected and one horn was flushed with warm M16 media. A set of representative images of the retrieved embryos are shown. See Table 3. (B) Histological analysis of day 4 pregnant uterine sections. Unflushed uterine horns were used for this experiment. Paraffin-embedded sections were stained with hematoxylin and eosin. lm, longitudinal

muscle; cm, circular muscle; s, stroma; le, luminal epithelium. Areas demarcated with a black rectangle are magnified in the right panels. Sections from two different Tsg101d/d uteri are shown as #1 and #2. Black arrowheads indicate distinct morphology of the luminal epithelia. The measurement of epithelial heights is shown in graph. Two sections from different subjects were chosen and heights of the luminal epithelia were measured in several different areas. Bars represent means ± SEM. (C) Immunofluorescence staining of E-cadherin (epithelial cell marker) and desmin (stromal cell marker). Unflushed uterine horns were used for this experiment. Areas demarcated with a white square are magnified in the lower panels. DNA was counterstained with TO-PROTM-3-Iodide (1:250).

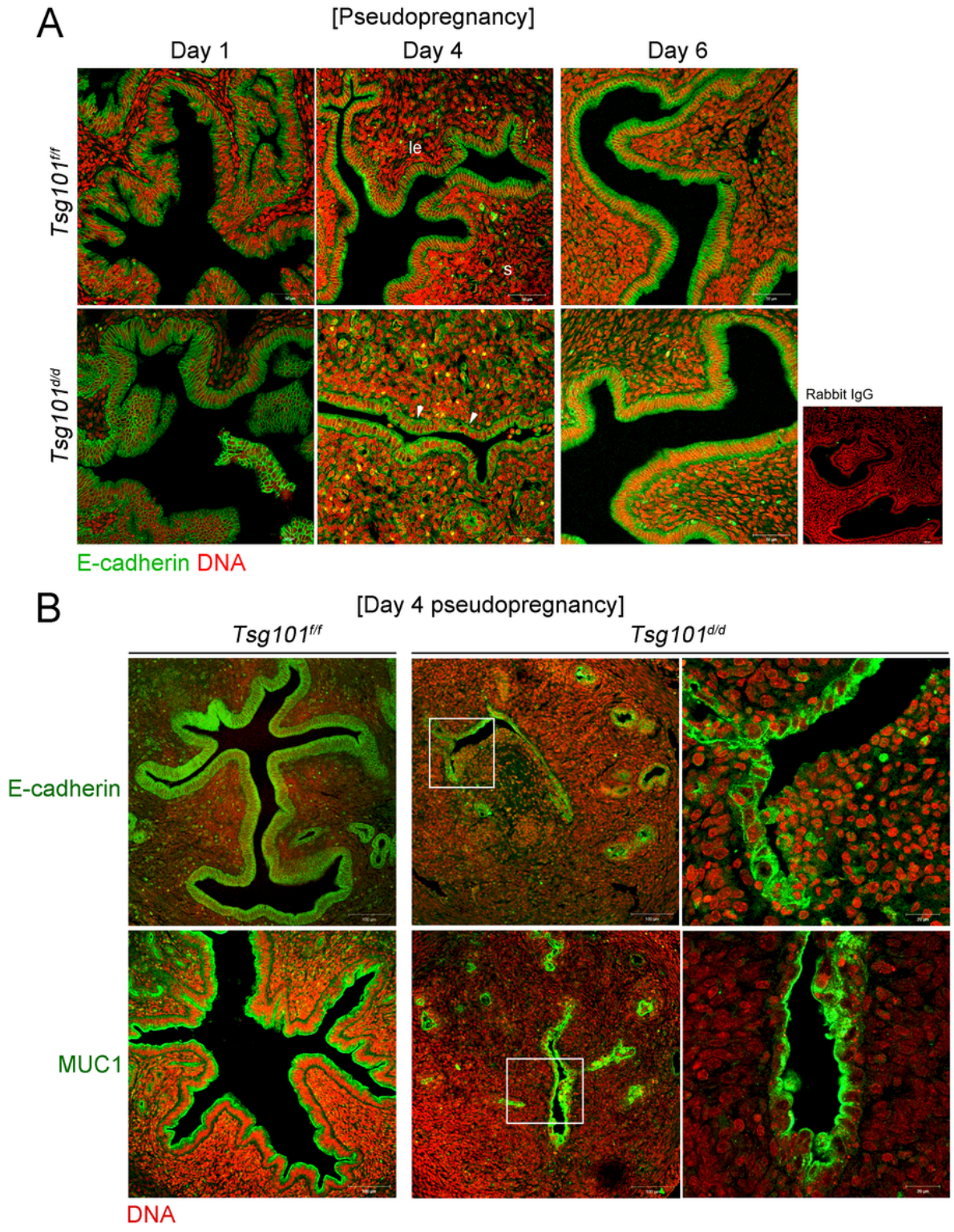

Figure 3

Immunofluorescence staining of E-cadherin and MUC1 in pseudopregnant Tsg101d/d uteri. (A) E-cadherin localization on day 1, 4, and 6 of pseudopregnancy. (B) E-cadherin and MUC1 localization in another set of day 4 pseudopregnant Tsg101f/f and Tsg101d/d uteri. The Tsg101d/d uterus shows disrupted luminal epithelial structure with abnormal E-cadherin and MUC1 localization pattern.

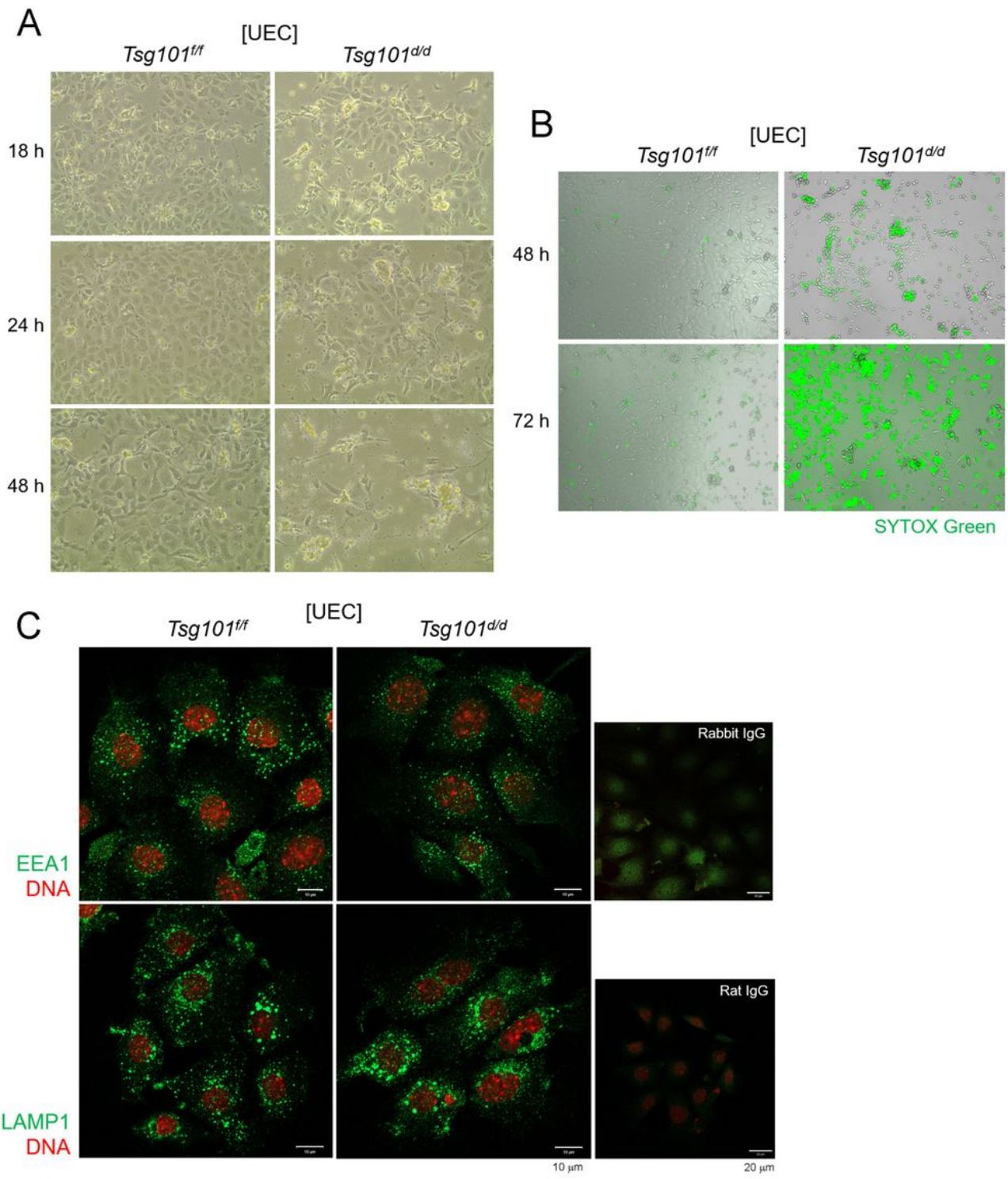

Figure 4

Tsg101d/d UECs gradually degenerate during in vitro culture. (A) UECs were isolated from Tsg101f/f and Tsg101d/d mice (11-week-old) and placed in culture at 2 × 105 cells per well. An injection of E2 was administered to the mice 24 h before sacrifice to increase the cell yield. The morphology of the cultured UECs was examined at the indicated times. (B) Live cell imaging of Tsg101f/f and Tsg101d/d UECs by using JuLITM FL. 48 h in culture, cells were stained with SYTOX Green, a live dye which stains DNA of

membrane-permeable cells (cells with weakened membrane or dead cells). (C) Immunofluorescence staining of EEA1 and LAMP1 in Tsg101f/f and Tsg101d/d UECs. UECs isolated from Tsg101f/f and Tsg101d/d mice (9-week-old) were cultured and subjected to immunofluorescence staining 18 h later. Cells were stained with indicated primary antibodies (green). DNA was stained with TO-PROTM-3-Iodine (1:250).

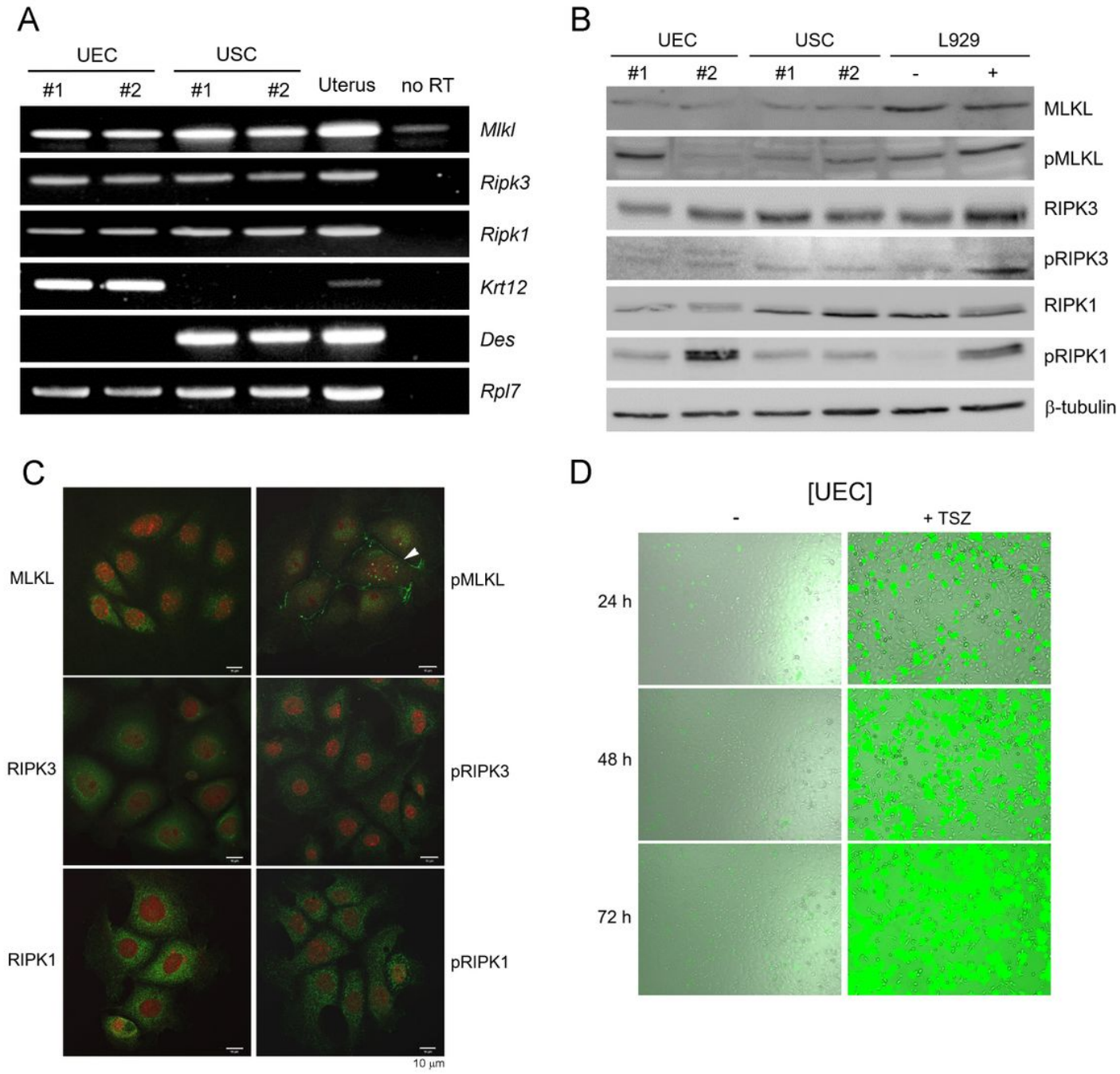

Figure 5

UECs express necroptosis effectors, RIPK1, RIPK3, and MLKL, and respond to necroptosis-inducing signal. (A) RT-PCR of necroptosis factors performed in isolated UECs, USCs, and uteri from random cycling ICR mice. E2 was given to mice 24 h before sacrifice to increase yield of UECs. Results from two

sets of independent samples experiments are shown as #1 and #2. RNA from whole uteri was used as a positive control. Mlkl, Mixed lineage kinase domain-like; Ripk3, Receptor interacting protein kinase 3; Ripk1, Receptor interacting protein kinase 1; Des, Desmin (a stromal marker); Krt12, Keratin 12 (an epithelial marker); Rpl7, Ribosomal protein L7 (a housekeeping gene). (B) Western blot analyses of necroptosis effectors in UECs and USCs. L929 cells treated with TSZ were used as a positive control. pMLKL, phospho-MLKL; pRIPK1, phospho-RIPK1; pRIPK3, phospho-RIPK3. (C) Immunofluorescence staining of necroptosis effects in cultured UECs. DNA was stained with TO-PROTM-3-Iodine (1:250). Experiments were repeated three times and a set of representative images are shown. (D) Isolated UECs were plated and treated with TSZ (TNFα + Smac mimetic LCL161 + zVAD-fmk) or DMSO (vehicle) the day after all cells had attached. TSZ was added at 24 h in culture along with SYTOX Green dye. Live images were captured at 1 h interval using the JuLIFM FL. TNFα, 30 ng/ml; Smac mimetic LCL161, 10 μM; zVAD-fmk, 20 μM.

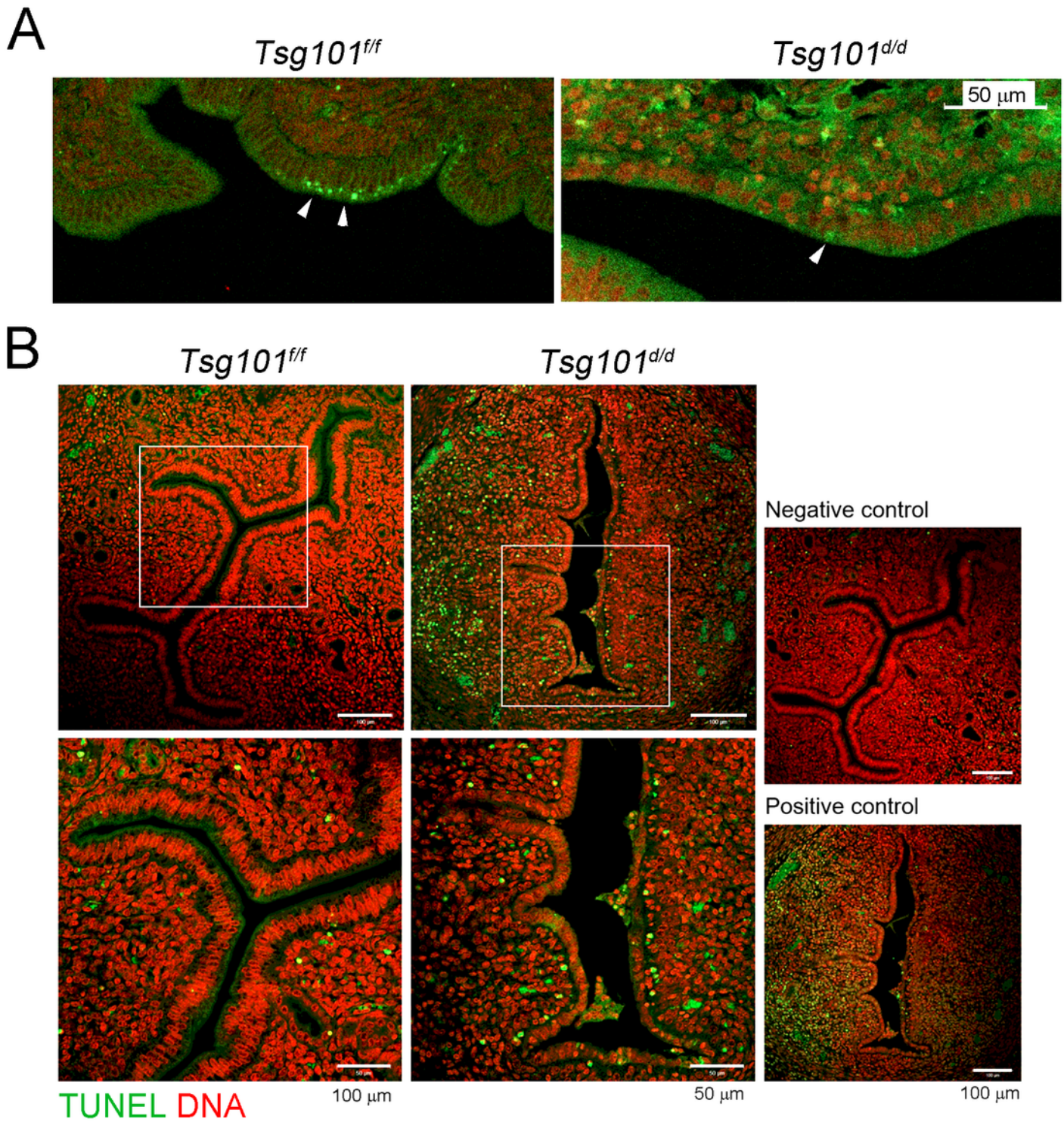

Figure 6

pMLKL immunofluorescence staining and TUNEL staining in Tsg101d/d uteri. (A) Immunofluorescence staining of pMLKL in day 4 pseudopregnant uteri. (B) TUNEL staining in day 4 pseudopregnant uteri to observe apoptotic cells. Green, apoptotic cell; red, nuclei. Areas demarcated with white rectangles are enlarged in the lower panel.

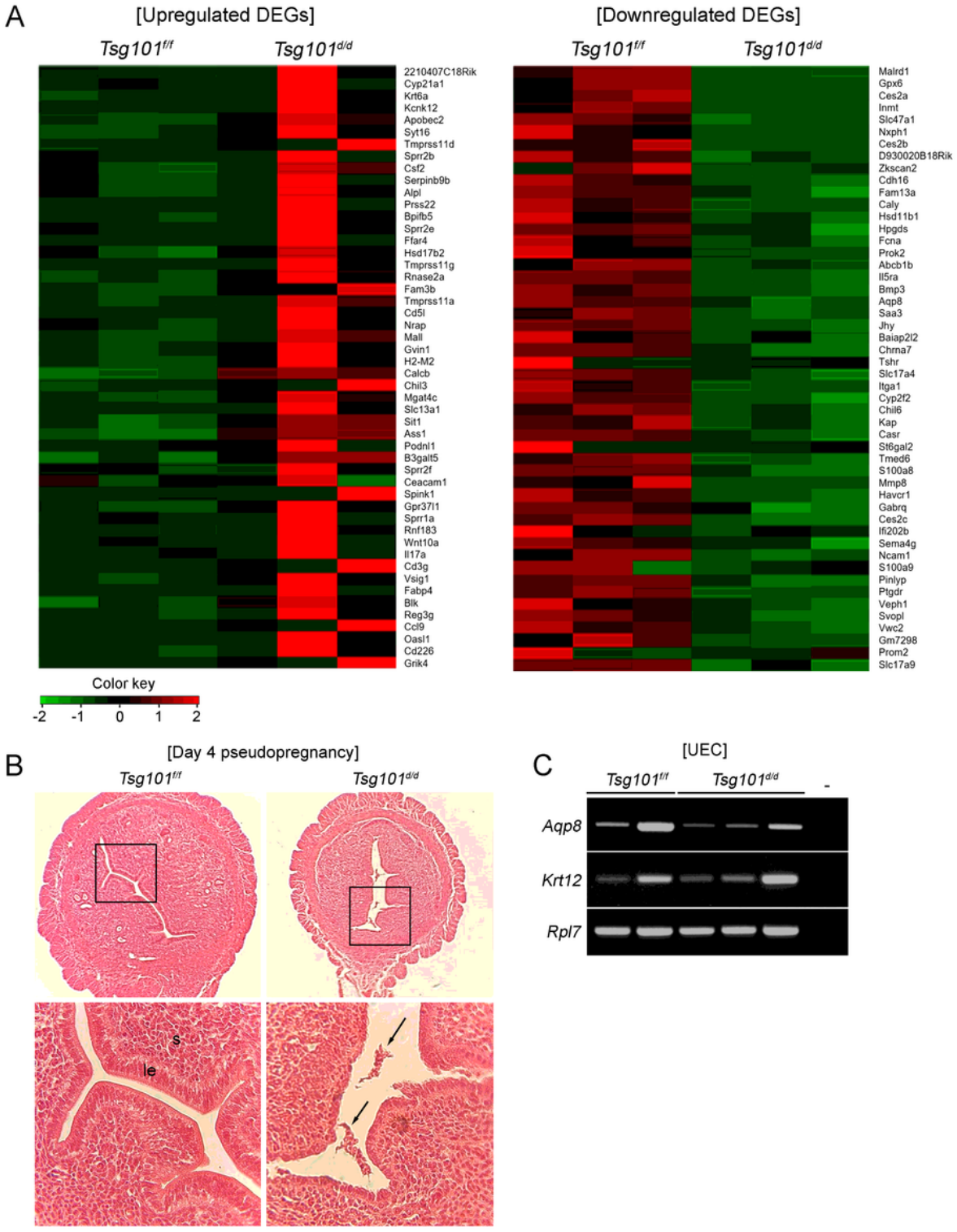

Figure 7

mRNA expression profiling in UECs from Tsg101f/f and Tsg101d/d mice. (A) Top 50 upregulated and downregulated genes are presented as heatmaps. (B) A representative histological image of day 4 pseudopregnant uteri used for mRNA expression profiling. Arrows indicate detached epithelial tissues in a Tsg101d/d uterus. le, luminal epithelium; s, stroma. (C) RT-PCR analyses of Aqp8 in UEC RNA samples. Two Tsg101f/f UEC and three Tsg101d/d UEC samples were used. -, no RT.

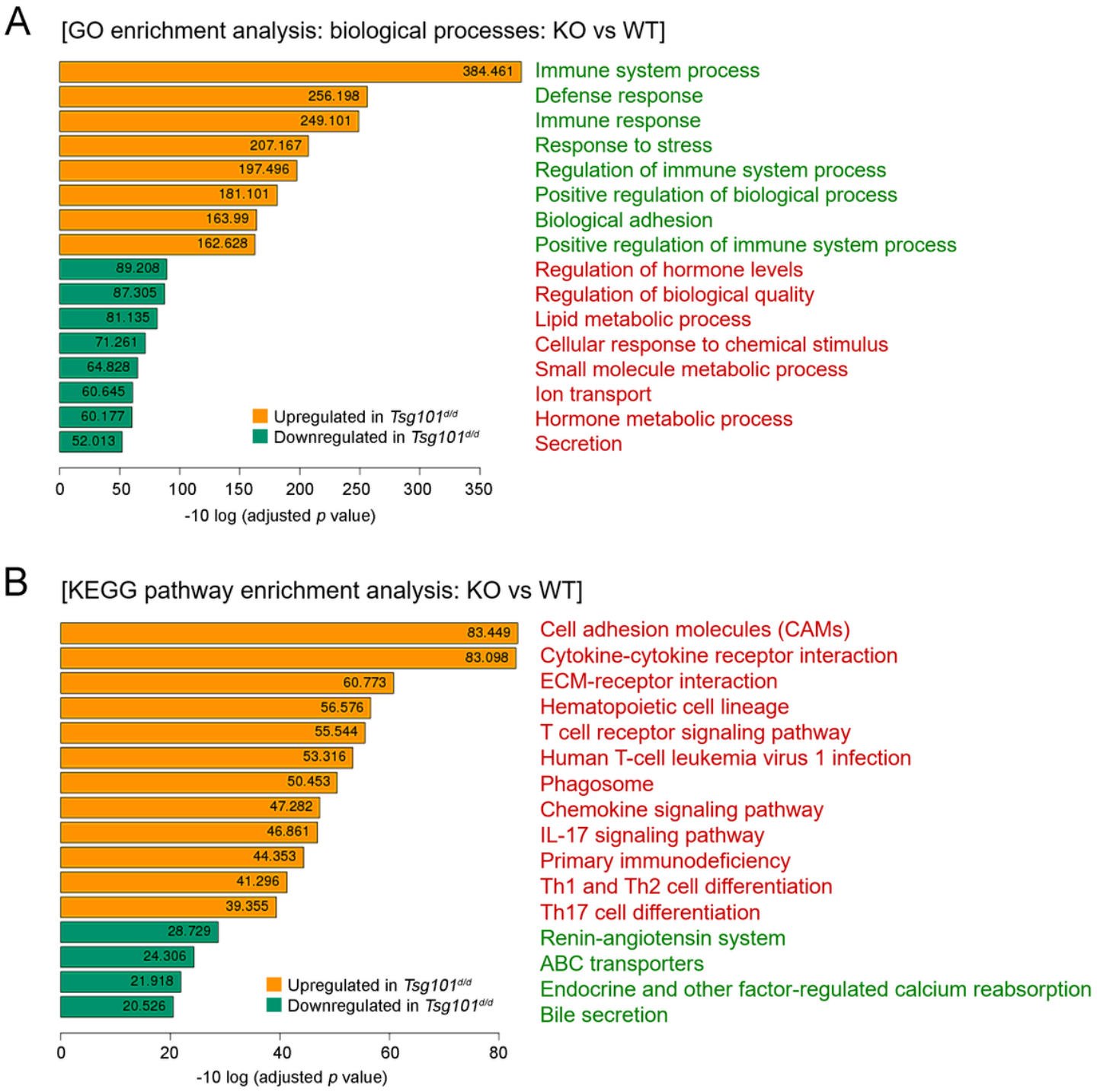

Figure 8

Pathway analyses of gene expression profiles. (A) Gene Ontology (GO) term enrichment analysis of biological processes for upregulated and downregulated DEGs between the Tsg101f/f and Tsg101d/d UECs. Top 16 GO terms associated with the biological processes are shown. The X-axis corresponds to the mean expression value of negative log 10 (adjusted p value). (B) Kyoto Encyclopedia of Genes and Genomes (KEGG) pathway enrichment analysis for the upregulated and downregulated genes between the Tsg101f/f and Tsg101d/d UECs. Gene expression information was mapped to the KEGG pathway

and the top 12 significantly upregulated and the top 4 downregulated pathways are shown. The X-axis corresponds to the mean expression value of negative log 10 (adjusted p value).